Spectrally condensed turbulence in thin layers

H. Xia,[1,a)] M. Shats,[1] and G. Falkovich[2]
[1]*Research School of Physics and Engineering, The Australian National University, Canberra ACT 0200, Australia*
[2]*Physics of Complex Systems, Weizmann Institute of Science, Rehovot 76100, Israel*

(Received 10 September 2009; accepted 10 November 2009; published online 18 December 2009)

We present experimental results on the properties of bounded turbulence in thin fluid layers. In contrast with the theory of two-dimensional (2D) turbulence, the effects of the bottom friction and of the spectral condensation of the turbulence energy are important in our experiment. Here we investigate how these two factors affect statistical moments of turbulent fluctuations. The inverse energy cascade in a bounded turbulent quasi-2D flow leads to the formation of a large coherent vortex (condensate) fed by turbulence. This vortex, depending on its strength, can substantially affect the turbulence statistics, even at small scales. Up to the intermediate strength of the condensate, the velocity moments similar to those in isotropic 2D turbulence are recovered by subtracting the coherent component from the velocity fields. A strong condensate leaves a footprint on the underlying turbulence; it generates stronger non-Gaussianity and reduces the efficiency of the inverse energy cascade. Remarkably, the energy flux in the cascade derived from the third-order structure function using the Kolmogorov flux relation gives physically meaningful values in a broad range of experimental parameters regardless of the condensate strength. This result has important implications for the analysis of the atmospheric wind data in upper troposphere and lower stratosphere. © *2009 American Institute of Physics*. [doi:10.1063/1.3275861]

I. INTRODUCTION

Turbulent flows in fluids whose depth is much less than their horizontal extent present both fundamental and practical interest since many natural and laboratory systems may, to some degree, be viewed as two dimensional (2D). To what extent a flow is quasi-2D depends on the aspect ratio of the system and can be influenced by other factors, such as rotation and stratification in neutral fluids, or magnetic field in plasma. Sometimes these factors coexist and complement each other, as for example in the planetary atmospheres, or in the ocean, where the depth of the flow can be much smaller than the horizontal scales, while the system also rotates.

Turbulence in an idealized 2D fluid was considered by Kraichnan[1] who showed that if turbulence is forced at some intermediate wave number k_f, spectral energy flows upscale, toward smaller wave numbers, $k<k_f$, while enstrophy (integral of squared vorticity) flows downscale, toward higher wave numbers, $k>k_f$, where it is dissipated by viscosity. The kinetic energy spectra are given by $E(k)=C\epsilon^{2/3}k^{-5/3}$ in the inverse energy cascade range, $k<k_f$, and by $E(k)=C_q\eta^{2/3}k^{-3}$ for the small scales, in the forward enstrophy cascade range, $k>k_f$. Here ϵ and η are the dissipation rates of energy and enstrophy, respectively, and C is the Kolmogorov constant. If no large-scale energy dissipation is present, energy cascades to larger and larger scales with no steady-state possible.

In the presence of the large-scale or uniform dissipation (e.g., bottom friction), energy delivered via the cascade will be dissipated. The maximum of the spectrum in this case will stabilize at some dissipation wave number given by $k_{\alpha_v}\approx 2\pi(\alpha_v^3/\epsilon)^{1/2}$, where α_v is the linear velocity dissipation rate. To achieve this steady state, the dissipation scale $2\pi/k_\alpha$ needs to be smaller than the system size L. This regime was studied experimentally[2,3] and numerically.[4,5] Energy spectra observed in the energy cascade range are close to the predicted $k^{-5/3}$ power law. Normalized higher-order moments (third and fourth) of turbulent velocity fluctuations suggest small non-Gaussianity and no signatures of the large-scale coherent structures.[3,5] The Kolmogorov constant is in the range of $C=5.6-7$ (see Ref. 5 and references therein).

Similar to three-dimensional (3D) turbulence, where the Kolmogorov flux relation relates the energy flux ϵ in the energy inertial range to the third-order velocity structure function S_3 (e.g., Refs. 6–8), in two dimensions this relation also holds $\epsilon=S_3/r$. The sign of S_3 is indicative of the direction of the energy cascade: positive S_3 corresponds to the inverse energy cascade (from small to large scales), while negative values indicate direct cascade.

If turbulence domain is bounded, spectral energy may start accumulating at the box size. In the system with linear dissipation this occurs when the dissipation scale exceeds the box size, $2\pi/k_\alpha>L$. This energy pileup at the scale close to the box size, referred to as spectral condensation, was predicted by Kraichnan and has been confirmed in numerical simulations[9–14] and experimentally.[3,15–18] In cases with zero damping (realized in numerics) the condensate grows.[10,11,14] When damping is present, the condensate is stabilized as a mean flow coherent over the system size and over many rotation periods, and the system as a whole achieves a statistically steady state.

The energy spectrum of the strong condensate deviates from the $k^{-5/3}$ power law, and it is close to $k^{-(3-4)}$ in both numerics[11,14] and in experiment.[16] Such a spectrum is suggested[14] to be due to the presence of a coherent structure

a)Electronic mail: hua.xia@anu.edu.au.

 © 2009 American Institute of Physics

Downloaded 20 Dec 2009 to 150.203.179.95. Redistribution subject to AIP license or copyright; see http://pof.aip.org/pof/copyright.jsp

and does not represent turbulent velocity fluctuations involved in the cascade. The subtraction of the mean flow recovers a spectrum of the underlying turbulence.[14,17,18] It has been shown[18] that in a broad range of the condensate strengths, the large-scale k^{-3} range coexists with the Kraichnan $k^{-5/3}$ energy cascade and k^{-3} enstrophy cascade ranges. It has also been shown that the spectral extent of the condensate and its strength depends on several factors, of which the most important are the system size and the bottom friction rate; the lower the bottom drag, the stronger the condensate for a given system size.

We arrive at an interesting dilemma in bounded quasi-2D system; the lower the bottom dissipation, the closer a system approaches idealized theoretical limit of the inertial range with no sources and sinks of energy. On the other hand, low dissipation in the presence of boundary inevitably leads to spectral condensation of turbulence and to the formation of strong coherent vortex (shear flow) which violates theoretical assumptions of the turbulence homogeneity and isotropy. This must be true in most of practical applications including planetary atmospheres and oceans, where one deals with systems of the finite size and nonzero bottom friction. The question is whether theoretical predictions of the Kolmogorov–Kraichnan theory are applicable beyond its main assumptions?

The Kolmogorov flux relation has been confirmed in numerical simulations,[5] and it has recently been used for the first time to measure ϵ in laboratory experiments.[17,18] In this paper we experimentally investigate the limits of its applicability in thin fluid layers in the presence of a strong dissipation in the energy cascade range, and also in the presence of spectral condensates of different strengths. We also study how the higher-order velocity moments in spectrally condensed 2D turbulence are modified by mean shear flows.

The paper is organized as follows. Section II describes the experimental setup, the phenomenology of spectral condensation, and effects of the bottom friction. In Sec. III we present the effects of spectral condensates of various strengths on the moments of turbulent velocity fluctuations. We show that the presence of a mean coherent flow changes different statistical moments in different ranges of scales and illustrate the importance of mean subtraction for the analysis of spectrally condensed turbulence. Similarities between velocity moments measured in laboratory thin fluid layers and in the Earth atmosphere are discussed. As the strength of the condensate flow is increased, the velocity moments of turbulence are affected more and more, showing substantial deviations from the isotropic 2D turbulence results. In Sec. IV we discuss experimental results and summarize the conclusions.

II. SPECTRAL CONDENSATION IN THIN FLUID LAYERS

A. Experimental setup

In our experiments, turbulence is generated electromagnetically in the stratified layers of fluids whose thickness does not exceed 4–5 mm. Two fluids with distinctly different properties are used. A heavier nonconducting fluid (Fluorinert FC-77, specific gravity SG=1.8) is placed at the bottom. A lighter conducting fluid, NaCl water solution (SG=1.03), is placed on top. Both layers of fluids are placed in the vertical magnetic field produced by a square matrix of 30×30 permanent magnets (10 mm apart). This matrix is placed either underneath the fluid cell, or it is submerged in the Fluorinert. Two carbon electrodes are used to drive electric current (up to 3 A) through the top layer. This current interacts with vertical magnetic field to generate 900 vortices ($\approx$9 mm in diameter) which produce turbulent quasi-2D flow. The electromagnetic forcing in this setup is detached from the bottom of the fluid cell, which helps to isolate the flow from the shear boundary layer. The dissipation due to the bottom drag can be controlled by changing the thickness of the fluid layers. The flow is limited by the walls of the fluid cell (0.3×0.3 m^2) and also by insertable square boundaries of the sizes $L=(0.09-0.24)$ m. Overall, the experimental setup is similar to previous experiments[3,17,19] but has a substantially larger number of forcing vortices, higher spatial resolution, and larger scale separation ($L/l_f\approx30$).

To visualize the flow, imaging particles (polyamid, 50 μm, SG=1.03) are suspended in the top fluid layer and are illuminated using a 1 mm laser sheet parallel to the free surface. Laser light scattered by the particles is filmed from above using video camera (2 Mpixel) or a high resolution still camera (12.8 Mpixel) in the fast shooting mode. In the latter case two lasers, green and blue, are pulsed for 20 ms consecutively with a delay of (20–150) ms in between. In each still camera frame, two laser pulses produce a pair of images (green and blue) for each particle. The frame images are then split into pairs of images according to the color. The velocity fields are obtained from these pairs of images using the cross-correlation particle image velocimetry technique. The velocity fields are measured every 0.33 s (at the camera shooting rate). For a better time resolution a video camera (25 fps) with a single laser is used.

The linear damping rate α is controlled by changing the thickness of the two fluid layers. Damping rates in the range of $\alpha=0.05-0.5$ s^{-1} are achieved. The energy density is calculated as

$$E_0=(2N^2)^{-1}\sum_{i=1}^{N}\sum_{j=1}^{N}v_{i,j}^2, \tag{1}$$

where N is the velocity grid size. A damping rate is estimated from the decay of the energy density after switching off the forcing at $t=t_0$: $E_t=E_{t_0}e^{-\alpha(t-t_0)}$.

To ensure that there is no significant ripple on the free surface of the fluid, we use a laser-reflection technique to measure spectra and the amplitude of the surface ripple. We find that at modest forcing used in our experiments the potential energy contribution (due to the ripple) is several orders of magnitude smaller than the kinetic energy of the flow related to horizontal velocities.

It should be noted that recent reports on intrinsic three dimensionality of the electromagnetically driven shallow flows[20] have not been confirmed in our experiments: 3D flow features were observed only for a single-layer electrolyte of thickness comparable to the forcing scale. Stratified fluid

Downloaded 20 Dec 2009 to 150.203.179.95. Redistribution subject to AIP license or copyright; see http://pof.aip.org/pof/copyright.jsp

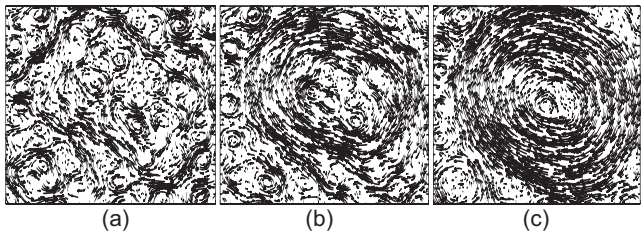

FIG. 1. Time-averaged velocity fields of the condensate in the square box of $L=0.1$ m at different thicknesses of the bottom fluid (Fluorinert FC-77): (a) $\Delta h_b=3$ mm, $\alpha=0.25$ s^{-1}, (b) $\Delta h_b=4$ mm, $\alpha=0.15$ s^{-1}, and (c) $\Delta h_b=5$ mm, $\alpha=0.05$ s^{-1}.

configurations with the layer thickness of less than 5 mm each do not show any 3D effects. The detailed results will be published elsewhere.

B. Generation of spectral condensate

Spectral condensation has been reported in the thin layer experiments[15,3,16] as the generation of a monopole vortex. We generate the condensate at three different linear damping rates within the square boundary of size $L=0.1$ m. Time-averaged (over 150 s) velocity fields of the flow after the emergence of the spectral condensate are shown in Fig. 1 for three different thicknesses of the bottom layer, $\Delta h_b=3,4$ and 5 mm. The time evolution of the energy density E_0 after forcing is switched off is shown in Fig. 2. These measurements are used to estimate the damping rates for different Δh_b. Damping plays a very important role for the symmetry of the condensate vortex. Table I summarizes parameters of the condensate flows for these three cases. The vortex turnover time is estimated using the maximum azimuthal velocity of the flow and the diameter of the vortex corresponding to this maximum velocity.

The condensate vortex becomes more symmetric as the vortex turnover time τ_{to} approaches the damping time $\tau_d \approx 1/\alpha$, as in Fig. 1(c). When τ_d is approximately one-third of the turnover time, the vortex is less symmetric, Fig. 1(b). For the least symmetric case of Fig. 1(a), the damping time is only 4 s comparing to an eddy turnover time of about 40 s.

It was proposed[14] that the spatial structure of the condensate vortex of Fig. 1(c) is universal. The circular vortex sucks energy from the turbulent background, which in turn is affected by the vortex due to the shear. It was suggested that the mean vorticity profile $\Omega(r)$, where $\Omega=\langle\nabla\times\vec{v}\rangle$, may scale as a function of the distance r from the center of the vortex: $\Omega(r)\sim r^{-\xi}$, where $1.2<\xi<1.33$.

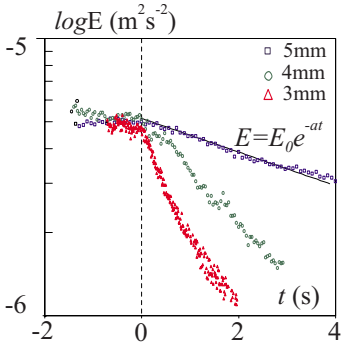

FIG. 2. (Color online) Decay of the energy density for cases Figs. 1(a)–1(c). The energy density is normalized to that of the case shown in Fig. 1(b) for comparison.

Figure 3 shows the mean vorticity profile calculated from our experimental data on the spectral condensate generated at $\Delta h_b=5$ mm within the boundary of $L\approx 0.1$ m at the linear damping coefficient of $\alpha=0.05$ s^{-1}.

The vorticity profile scales close to $r^{-1.25}$ (though the scatter is substantial), which falls within the theoretically predicted range and practically coincides with the scaling obtained in numerical simulations.[14] Thus the spatial structure of the condensate vortex may indeed be universal.

Regardless of the (a)symmetry of the condensate vortex (Fig. 1), the kinetic energy spectra of condensed turbulence are quite robust. To better resolve different spectral ranges in condensed turbulence, we perform measurements in a larger box, $L=0.235$ m. The kinetic energy spectrum of the flow obtained at $\alpha=0.16$ s^{-1} is presented in Fig. 4.

The spectrum shows three distinct spectral ranges characterized by different power-laws: $E(k)\sim k^{-m}$, where $m=(3-4)$, at large scales, $k<k_t$, and at small scales, $k>k_f$. In the intermediate range, $k_t<k<k_f$, the spectrum is close to the Kraichnan energy inertial range $E(k)\propto k^{-5/3}$. We will refer to these three ranges as to the *condensate range*, $k<k_t$, the *inverse energy cascade range*, $k_t<k<k_f$, and the *enstrophy cascade range*, $k>k_f$. Here $k_f=760$ m^{-1} is the wave number corresponding to the forcing scale. The Kolmogorov scale $\eta\sim\nu^{1/2}(\epsilon k_f^2)^{-1/6}$ is estimated to be around 1 mm in our experimental conditions, giving $k_\eta\sim 6000$ m^{-1} much larger than k_f.

It has been shown[18] that the strength and the spectral extent of the condensate, given by the position of the knee in the spectrum, k_t, Fig. 4, depend mostly on the size of the boundary, $k_t\propto L^{-3/2}$, the bottom drag energy dissipation, $k_t\propto\alpha^{-3/4}$, and, much weaker, on the energy injection rate, $k_t\propto\epsilon^{1/4}$. In the experiment we control the strength of the condensate relative to the $k^{-5/3}$ turbulence by changing L and α.

We characterize the strength of the spectral condensate by a ratio of the condensate energy to the total energy of the flow $A=E_{\rm cond}/E_0$. The condensate energy is computed from the time-averaged velocity field as

$$E_{\rm cond}=(2N^2)^{-1}\sum_{i=1}^{N}\sum_{j=1}^{N}\bar{V}_{i,j}^2, \tag{2}$$

where N is the velocity grid size. The time-averaged velocity field is computed by averaging a large number ($n_t=300-500$) of instantaneous full velocity fields, $\bar{V}(x,y)=(1/n_t)\Sigma_{n=1}^{n_t}V(x,y,t_n)$, such that turbulent velocity fluctuations average out, and the remaining velocity vectors represent mean coherent flow. The total energy density of the flow, E_0, is computed using full velocity fields, as explained in Sec. II A. For isotropic 2D turbulence, $A=0$.

The kinetic energy spectra were computed as follows. The Fourier transform of the 2D velocity field $u_i(x_n,y_m,t)$, where $i=x,y$, $n=1,2,\ldots,N$ and $m=1,2,\ldots,M$, is given by

Downloaded 20 Dec 2009 to 150.203.179.95. Redistribution subject to AIP license or copyright; see http://pof.aip.org/pof/copyright.jsp

TABLE I. Effect of linear damping.

Δh_b (mm)	α (s^{-1})	Maximum vortex velocity (m/s)	Vortex diameter (m)	τ_{to} (s)	$1/\alpha$ (s)
3	0.25	0.003	0.04	42	4
4	0.15	0.006	0.04	21	7
5	0.05	0.01	0.06	19	20

$$F_i(k_p,k_q)=\sum_{n=1}^{N}\sum_{m=1}^{M}u_i(x_n,y_m)e^{-i2\pi(pn+qm)}, \tag{3}$$

where $p=1,2,\ldots,N$ and $q=1,2,\ldots,M$. The power spectrum is $|F_i|^2=F_i(k_p,k_q)F_i^*(k_p,k_q)$, where * denotes complex conjugate.

A 2D kinetic energy spectrum is computed as $E(k_x,k_y)=|F_x|^2+|F_y|^2$ to generate a 1D energy spectrum,

$$E_k=\sum_{k=(k_x^2+k_y^2)^{1/2}}E(k_x,k_y). \tag{4}$$

The integral of this spectrum is then normalized by the energy density E_0 computed in physical space:

$$\int_0^\infty E_k dk=E_0=(2N^2)^{-1}\sum_{i=1}^{N}\sum_{j=1}^{N}v_{i,j}^2. \tag{5}$$

Such a normalization ensures that the kinetic energy of the flow derived from the velocity fields and from the spectra is the same. However, in the presence of the spectral condensate, this normalization can lead to an underestimation of the spectral energy in the inverse cascade range. Since in physical space the condensate represents a coherent vortex, the Fourier spectrum of this singular nonperiodic structure cannot accurately reproduce its spectral width and the amplitude. As a result $\int_0^{k_t}E_k dk$ appears to be larger than the real condensate energy E_{cond}. The normalization, Eq. (5), leads to the reduction in the spectral energy density not just at $k<k_t$, but also in the energy cascade range, such that E_k at $k>k_t$ becomes underestimated. It will be shown in Sec. III that the subtraction of the mean flow from the instantaneous velocity fields eliminates this problem and the correct value of E_k is then obtained. We also perform the energy balance analysis in the physical space rather than in the spectral domain to avoid this normalization problem. Naturally, the Fourier representation is inconvenient in the presence of an inhomogeneous mean flow.

III. STATISTICAL VELOCITY MOMENTS IN CONDENSED TURBULENCE

In this section we study statistical moments of the velocity increments across a distance r in a flow, $\delta v(\mathbf{r})=v(l+\mathbf{r})-v(l)$, where l denotes a position in the flow. Statistical moments of these increments, also referred to as structure functions of the order n, are computed as $S_n(\mathbf{r})=\langle[\delta v(\mathbf{r})]^n\rangle$. Here angular brackets denote averaging over all possible positions l within the flow field. To improve statistics we also perform averaging in time over many realizations of the instantaneous velocity fields. As mentioned in the Introduction, spectral energy flux through the inertial range in isotropic homogeneous 2D turbulence can be estimated from the Kolmogorov flux relation using the third-order structure function (e.g., Refs. 7 and 8),

$$S_3=(\langle(\delta V_L)^3\rangle+\langle\delta V_L(\delta V_T)^2\rangle)/2=\epsilon r,\quad r\gg 2\pi/k_f. \tag{6}$$

Here indices "L" and "T" stand for the longitudinal and transverse velocity components with respect to $\mathbf{r}$. Correspondingly, we will refer to the longitudinal S_{nL} and transverse S_{nT} structure functions. For S_3 in the 2D energy cascade range, the relation between longitudinal and transverse structure function is given by $S_3=(S_{3L}+S_{3T})/2$ and (see Ref. 7 and references therein)

$$S_{3L}=3S_{3T}. \tag{7}$$

The Kolmogorov flux relation has been confirmed in numerical simulations of 2D turbulence.[5] It allows the spectral energy flux ϵ to be estimated from the measured third-order structure function S_3.

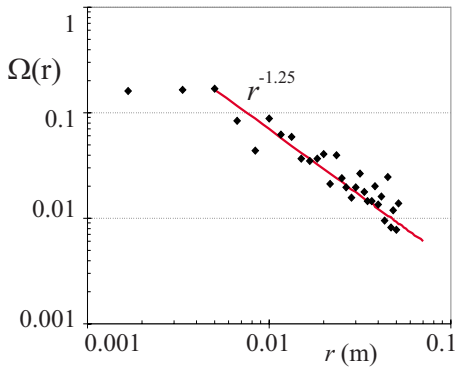

FIG. 3. (Color online) Radial profile of the mean vorticity field of the condensate in the square box of $L\approx 0.1$ m at $\Delta h_b=5$ mm, $\alpha=0.05$ s^{-1}.

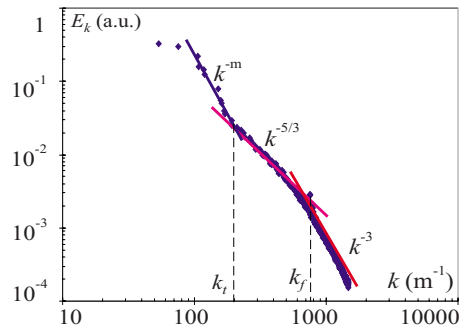

FIG. 4. (Color online) The kinetic energy spectrum of the flow at $L=0.235$ m and $\alpha=0.16$ s^{-1}.

Downloaded 20 Dec 2009 to 150.203.179.95. Redistribution subject to AIP license or copyright; see http://pof.aip.org/pof/copyright.jsp

Despite its practical importance, this method of ϵ estimation had not been successful in laboratory experiments. To achieve converged values of the odd-order velocity moments in experiment, large statistics is needed due to the cancellation of the positive and negative δv^{2n+1}.[3] The asymmetry in the probability density function of δv^3 is small in 2D turbulence and it is related to the value of skewness, or the third normalized velocity moment, $Sk=S_{3L}/(S_{2L})^{3/2}$, which in isotropic turbulence is of the order of $Sk\sim 0.04$. Below we show that the improved spatial and dynamic resolution of the velocity measurements and large statistical averaging in our experiment allowed for a reliable determination of the third-order structure function and ϵ. We also investigate if the Kolmogorov flux relation holds in the presence of a strong condensate.

A low value of skewness and flatness $F=S_{4L}/(S_{2L})^2$, obtained in numerical simulations of 2D turbulence[5] in experiments,[3] and also in numerical modeling of the growing condensate,[10,11] is interpreted as a sign that the statistics of 2D turbulence may be closer to Gaussian, in distinction from 3D turbulence. Here we will look for the signatures of non-Gaussianity in the constantly forced steady-state turbulence in the presence of spectral condensates of different strengths.

In this section we compare statistical properties of weak, intermediate, and strong condensates. These three cases correspond to the condensate strength parameters of $A=(0.2-0.4)$ (weak), 0.61 (intermediate), and 0.78 (strong).

A. Weak condensate

First we consider the case of a weak condensate $A=(0.2-0.4)$ obtained within the boundary of $L=0.235$ m at a relatively high linear damping of $\alpha\approx 0.3$ s^{-1}. As shown in Fig. 1(a), when the linear damping is high, the damping time is much larger than the eddy turnover time. As a result, the spectral condensate is not symmetric and is slowly varying in time. This gives rise to an uncertainty in determining the condensate strength. In this case, $A=(0.2-0.4)$ is obtained using different time averaging in Eq. (2).

The energy spectrum [Fig. 5(a)] shows minor differences compared to that of a homogeneous isotropic turbulence. A spectral range between the forcing scale wave number $k_f\approx 760$ m^{-1} and $k_t\approx 150$ m^{-1} shows a power-law scaling close to $k^{-5/3}$, while at lower wave numbers $k<k_t$, it is steeper. Both skewness, $Sk=(0.03-0.1)$, and flatness, $F=(3-3.3)$, of the velocity fluctuations are close to their values in isotropic 2D turbulence. The variation in skewness for different r in the energy cascade range is possibly due to the high damping rate which we will discuss later.

The third-order structure function [Fig. 5(b)] is positive, in agreement with the expectations of the inverse energy cascade. S_3 is a linear function of r, at least in the range $r<2\pi/k_t\approx 0.04$ m, which corresponds to the $k^{-5/3}$ part of the energy spectrum. The energy flux calculated (by extrapolating to $r\gg 2\pi/k_f$) for this range is $\epsilon\simeq 7\times 10^{-6}$ m^2 s^{-3}. The longitudinal component S_{3L} is approximately three times higher than the transverse one S_{3T}, in agreement with theoretical expectations, Eq. (7).

The weak condensate does not seem to change much

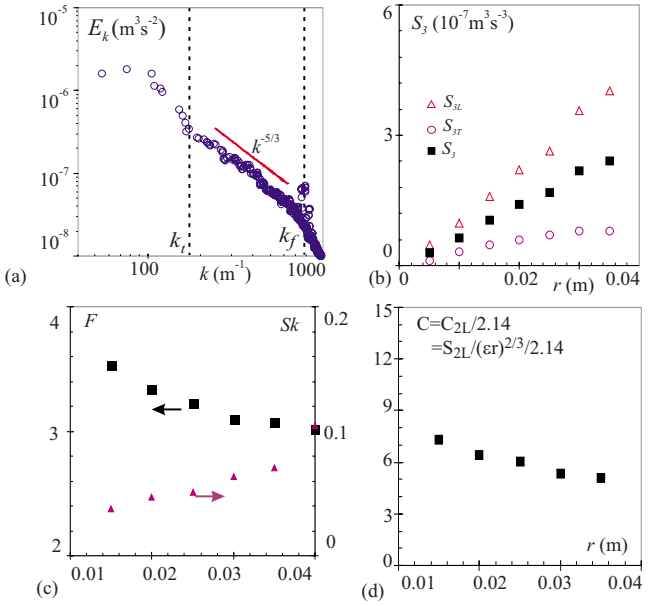

FIG. 5. (Color online) Weak spectral condensate in the $L=0.235$ m boundary box, linear damping coefficient $\alpha\approx 0.3$ s^{-1}. (a) Energy spectrum, (b) longitudinal (triangles), transverse (circles) and full (squares) third-order structure functions, (c) flatness (squares) and skewness (triangles), and (d) Kolmogorov constant C calculated from C_{2L} as functions of the separation distance r.

statistical moments of turbulent velocity fluctuations. The spectrum, the direction (given by positive S_3), and the value of the spectral energy flux are consistent with the 2D turbulence theory and with the expectation of the inverse energy cascade.

The Kolmogorov constant $C=E(k)\epsilon^{-2/3}k^{5/3}$, which relates the spectral energy density, $E(k)$, the energy flux in the cascade range, ϵ, and the wave number, k, can also be estimated using the physical space parameters by calculating the second-order structure function constant.[5] In the next section (Sec. III B) we will compare the values of C estimated from the spectral domain (after mean subtraction) and from the physical space. Here we compute the longitudinal structure function of the second order S_{2L} in the inverse energy cascade range and the corresponding structure function constant $C_{2L}=S_{2L}(r)/(\epsilon r)^{2/3}$, shown in Fig. 5. The Kolmogorov constant is related to this quantity as $C_{2L}=2.14C$ (see Ref. 5 for details). In our experiment $C_{2L}\approx 12.5$ in the energy cascade range. This gives the Kolmogorov constant of $5<C<7$ in the energy cascade range. This is close to the value of $C=(5.6-7)$ obtained in numerical simulations of isotropic 2D turbulence.[5]

The value of the energy flux derived from Fig. 5(b) ($\epsilon\simeq 7\times 10^{-6}$ m^2 s^{-3}) has been compared with the energy balance estimates derived from the time evolution of the energy density of the flow. The evolution of the total energy density is given by

$$\frac{dE}{dt}+\alpha E=\epsilon_i, \tag{8}$$

where ϵ_i is the energy flux injected into the flow at the forcing scale.

Downloaded 20 Dec 2009 to 150.203.179.95. Redistribution subject to AIP license or copyright; see http://pof.aip.org/pof/copyright.jsp

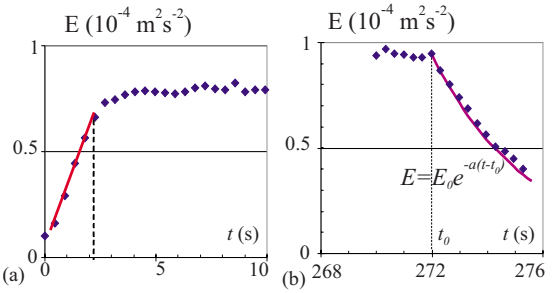

FIG. 6. (Color online) Evolution of the total energy density of the flow (a) right after switching on the forcing and (b) during the decay stage (conditions of weak spectral condensate).

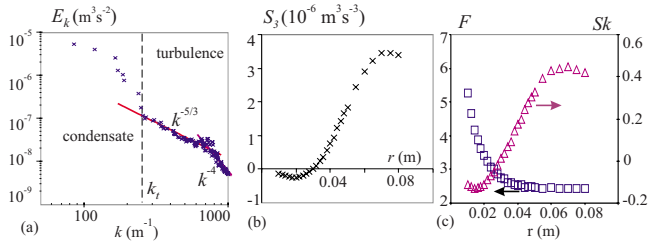

FIG. 7. (Color online) Intermediate-strength spectral condensate in the $L=0.15$ m boundary box, linear damping $\alpha \approx 0.15$ s^{-1}. (a) Energy spectrum, (b) the third-order structure function, and (c) flatness (squares) and skewness (triangles) as functions of the separation distance r.

The measured $E(t)$ is shown in Fig. 6. Shortly after the current is switched on, energy grows linearly with time Fig. 6(a). During this interval of time the inverse energy cascade broadens the turbulence spectrum from initially narrow peak at $k=k_f$ toward the lowest wave number. Initially the energy density is low, such that $\alpha E \ll \epsilon_i$. The rate of growth $dE/dt \approx 2.7\times 10^{-5}$ m^2 s^{-3} in the early stage of the turbulence evolution thus gives an estimate of ϵ_i.

The decay of the total energy density after the current is switched off at $t=t_0$ is used to estimate the energy dissipation rate. As shown in Fig. 6(b), the energy density of the flow decays exponentially after switching off the forcing in agreement with $\partial E/\partial t|_{t\geq t_0}=-\alpha E$, which gives $E=E_0e^{-\alpha(t-t_0)}$, where E_0 is the total energy density of the flow at $t=t_0$. The energy dissipation rate for $\alpha=0.3$ s^{-1} and $E_0=9.2\times 10^{-5}$ m^2 s^{-2} is given by $\alpha E_0=2.7\times 10^{-5}$ m^2 s^{-3}, which in the steady state ($dE/dt=0$) balances the injected energy flux.

The energy dissipation by turbulent fluctuations ϵ_d is smaller than the total dissipation rate by a factor of $(1-A)$: $\epsilon_d \approx \alpha E_{\rm turb}=(1-A)\alpha E_0$, assuming negligible viscous dissipation. The energy flux injected into the flow at the forcing scale is dissipated by turbulence (ϵ_d) and by the condensate ($\epsilon_c \approx A\alpha E_0$): $\epsilon_i=\epsilon_d+\epsilon_c$. In this case, $\epsilon_c=(5.4-10)\times 10^{-6}$ m^2 s^{-3}. The energy flux of $\epsilon=7\times 10^{-6}$ m^2 s^{-3} calculated from $S_3(r)$ appears to be in agreement with ϵ_c. The agreement is in fact even better for the cases with lower damping (see below). The ratio of the energy dissipation by turbulence to the injected energy flux is $\epsilon_d/\epsilon_i=1-A=(0.6-0.8)$ for the weak condensate and it is 0.39 and 0.22 for the intermediate and strong condensates, correspondingly. In other words, the energy flux dissipated by turbulent fluctuations in the energy cascade range constitutes a substantial fraction of the energy flux injected by the forcing into the flow. This indicates that the energy cascade spectral range is not strictly speaking an inertial range. Nevertheless these and previous experiments confirm good agreement with the 2D turbulence theory.

It is difficult to keep the bottom dissipation low and at the same time avoid strong spectral condensation. When the bottom dissipation is further increased (by decreasing the thickness of the fluid layers), the condensate disappears, but the spectrum in the energy cascade range changes its scaling from $k^{-5/3}$ to a flatter one, $E(k)\propto k^{-1}$, due to the fact that the energy flux becomes strongly affected by the bottom damping and changes substantially within the energy cascade range. This problem is also well recognized in numerical simulations of 2D turbulence (e.g., Refs. 5 and 21–23). To avoid the condensation and to keep the energy cascade range free of sources and sinks in numerical simulations, the large scale dissipation is often introduced only at the largest scales (infrared damping). The introduction of the linear dissipation in the numerical model of Ref. 5 stopped the development of the condensate, but did not strongly affect the turbulence spectra, nor the higher-order structure functions, in agreement with our results. Thus we can conclude that recently expressed concerns[24] that the presence of strong dissipation in the energy cascade range renders any comparisons between experiments and the theory of 2D turbulence invalid are not justified.

B. Intermediate condensate

A condensate of an intermediate strength ($A=0.61$) is generated within a smaller boundary, $L=0.15$ m, and at lower damping, $\alpha \approx 0.15$ s^{-1}. In this case the energy spectrum also shows three different power laws: $E_k \propto k^{-(3-4)}$ for small and large scales and $k^{-5/3}$ in the intermediate range of wave numbers, $k_t<k<k_f$, Fig. 7(a). The third-order structure function, however, changes dramatically in this case. S_3 becomes negative in the range of scales $2\pi/k_f<r<2\pi/k_t$, while at larger scales, $r>2\pi/k_t$, S_3 is positive, and the $S_3(r)$ dependence is not linear as seen in Fig. 7(b). Flatness and skewness are shown in Fig. 7(c). These normalized moments show much larger variability with r compared to the weak condensate. Since turbulence in these experiments is forced at small scales, negative S_3 cannot be indicative of the direct (downscales) cascade. The change in S_3 compared to the weak condensate case must be attributed to the formation of the large-scale mean shear flow resulting from spectral condensation.

Indeed, in the presence of the spectral condensate, the flow velocity and its increments contain both mean and fluctuating velocity components, $\delta V=\delta\bar{V}+\delta\tilde{V}$. The second-order structure function contains not only second moment of velocity fluctuations $\delta\tilde{V}^2$, but also two other terms, $\langle\delta V^2\rangle=\langle\delta\bar{V}^2+2\delta\bar{V}\delta\tilde{V}+\delta\tilde{V}^2\rangle$. The second term averages out. The third-order moment is affected more: $\langle\delta V^3\rangle=\langle\delta\bar{V}^3-3\delta\bar{V}^2\delta\tilde{V}+3\delta\bar{V}\delta\tilde{V}^2-\delta\tilde{V}^3\rangle$. Again, a term which contains $\delta\tilde{V}$ averages

Downloaded 20 Dec 2009 to 150.203.179.95. Redistribution subject to AIP license or copyright; see http://pof.aip.org/pof/copyright.jsp

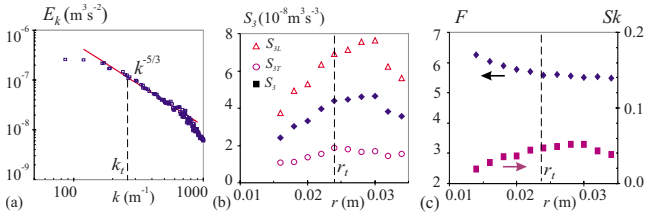

FIG. 8. (Color online) (a) Energy spectrum, (b) longitudinal (triangles), transverse (circles) and full (squares) third-order structure functions, and (c) normalized velocity moments F and Sk computed after the subtraction of the mean flow from $N=350$ instantaneous velocity fields in the intermediate condensate case. Vertical dashed lines indicate the wave number and the scale corresponding to the knee in the spectrum of Fig. 7(a).

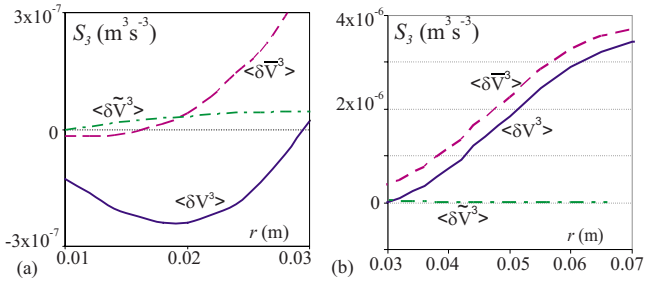

FIG. 10. (Color online) S_3 calculated using the full velocity $\langle \delta V^3 \rangle$, mean velocity $\langle \delta \bar{V}^3 \rangle$, and the fluctuation velocity $\langle \delta \tilde{V}^3 \rangle$ at scales from (a) 0.01 m to 0.03 m and (b) from 0.03 m to 0.07 m.

to zero, while the terms $\langle \delta \bar{V}^3 \rangle$ and $\langle 3\delta \bar{V} \delta \tilde{V}^2 \rangle$ modify the third velocity moment in the presence of the mean shear flow.

To recover statistical moments and spectra of underlying turbulence from the measured total velocity fields, we subtract mean time average velocity $\bar{V}(x,y) = (1/n_t)\Sigma_{n=1}^{n_t} V(x,y,t_n)$ from n_t instantaneous velocity fields and repeat the above analysis. Figure 8 shows the results. The energy spectrum now shows $E(k) \propto k^{-5/3}$ power law over (almost) the entire spectral range, Fig. 8(a). The scatter in the spectrum after mean subtraction is reduced compared with Fig. 7(a). This actually supports the suggestion that even the second moment is "polluted" by the mean $\langle \delta \bar{V}^2 \rangle$ component of the flow.

The third-order structure function is positive in the energy cascade range of scales, Fig. 8(b). At scales corresponding to $2\pi/k_f < r < 2\pi/k_t$, S_3 is a linear function of r. The spectral energy flux in this range is estimated as $\epsilon = S_3/r$. The value of the Kolmogorov constant, derived from the second-order structure function constant (see Sec. III A), is higher than in the weak condensate case [shown in Fig. 9(a)], $C \approx 7$, but is still close to the numerical simulation results.

Figure 8(c) shows flatness and skewness in this regime after mean subtraction. In the presence of the stronger condensate, skewness at scales larger than the forcing scale is small but positive, $Sk=(0.02-0.05)$. Flatness $F \approx 5.5$ however is noticeably higher than in the weak condensate regime.

As discussed in Sec. II B, after the mean flow is subtracted, the Kolmogorov constant can be estimated as $C = E_k \epsilon^{-2/3} k^{5/3}$. Figures 9(a) and 9(b) show the Kolmogorov constant estimated from the structure function and from the spectral energy and ϵ. In both cases $C=(6-7)$ in the energy cascade range, in agreement with the isotropic 2D turbulence results.

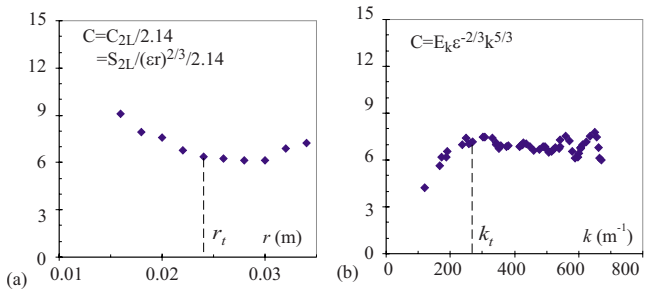

FIG. 9. (Color online) The Kolmogorov constant deducted from (a) second order structure function constant C_{2L} as $C=C_{2L}/2.14=S_{2L}/(\epsilon r)^{2/3}/2.14$ and (b) energy spectrum as $C=E_k\epsilon^{-2/3}k^{5/3}$, after the subtraction of the mean flow from $N=350$ instantaneous velocity fields in the intermediate condensate case.

Let us consider which terms dominate different scales in $\langle \delta V^3 \rangle = \langle \delta \bar{V}^3 + 3\delta \bar{V} \delta \tilde{V}^2 - \delta \tilde{V}^3 \rangle$. To compare these terms, we show S_3 calculated using the full velocity $\langle \delta V^3 \rangle$, the mean velocity $\langle \delta \bar{V}^3 \rangle$, and the fluctuation velocity $\langle \delta \tilde{V}^3 \rangle$ as functions of r in Fig. 10. It is clear that the mean velocity $\langle \delta \bar{V}^3 \rangle$ is dominant at large scales (from 0.04 to 0.07 m), while at small scales (0.01 to 0.03 m), negative S_3 is caused by the cross term $\langle 3\delta \bar{V} \delta \tilde{V}^2 \rangle$.

C. Similarities with atmospheric turbulence

The results presented above can possibly reopen a long standing debate regarding the origin of the spectra of atmospheric turbulence. The spectra of kinetic energy of atmospheric winds have been analyzed during the Global Atmospheric Sampling Program.[25] These wave number spectra measured in the upper troposphere and in the lower stratosphere have shown two power laws: $E(k) \propto k^{-5/3}$ for the scales between 10 and 500 km and a steeper spectrum with $E(k) \propto k^{-3}$ in the range of scales (500–3000) km (similar to the spectrum of Fig. 4). The observation of the same two power laws as in isotropic 2D turbulence[1] but in the reverse order triggered numerous hypotheses on the origin of the $k^{-5/3}$ mesoscale range, such as 2D turbulence with two sources of energy in which the inverse energy cascade from the small-scale forcing arises from a strong convection,[26] or a breakup of internal gravity waves.[27] The large-scale part of the spectrum can be due to a direct vorticity cascade,[26] or it can result from an inverse cascade of inertio-gravity waves.[28] It can also result from an energy pile up at the system scale in the process of spectral condensation as in numerics[11] and in our experiment.

Since the $k^{-5/3}$ power law can either be due to the inverse energy cascade in 2D turbulence, or due to the direct cascade in 3D, a third order structure function $S_3(r)$ was computed based on the MOSAIC atmospheric database which accumulated wind velocities measured on 7630 aircraft flights.[29] This function was found negative in the range of scales between 10 and 100 km. Also S_3 was not a linear function of r.

Downloaded 20 Dec 2009 to 150.203.179.95. Redistribution subject to AIP license or copyright; see http://pof.aip.org/pof/copyright.jsp

It was concluded that the negative S_3 contradicted the existence of the inverse energy cascade. The negativity of the third moment spawned hypotheses about a direct energy cascade in a two-layer model or stratified turbulence simulations.[30,31] However, Ref. 32 questioned the two-layer model[33] and noted potential pitfalls in the interpretation of the results.

In light of the results presented above, the conclusions about the evidence of the direct cascade and its 3D nature may need to be reconsidered. To establish whether the cascade in the mesoscale range is direct or inverse, one needs to reanalyze the atmospheric data in the way described here: subtract mean flows, which are certainly present in atmosphere, and determine separately the second and the third moments of the velocity fluctuations. Let us stress that it is irrelevant whether the large-scale flows are generated by the inverse cascade or by any other large-scale source. They distort small-scale turbulence just the same and need to be subtracted to analyze the flux and other high moments. Arguments in support of the atmospheric turbulence described as 2D turbulence with a condensate[11] agree with the results presented here.

It is important to note that the second and the third velocity moments may be affected by the mean shear flows in different ranges of scales r. Let δv and δV be small- and large-scale parts of the velocity difference, respectively. Comparing $\langle(\delta V)^2\rangle \cong s^2 r^2$ with $\langle(\delta v)^2\rangle \cong C(\epsilon r)^{2/3}$, we see that the small-scale (turbulent) part dominates at the scales smaller than $l_t \cong C^{3/4} s^{-3/2} \epsilon^{1/2}$. Here $s = V/L_s$ is a large-scale velocity gradient and L_s is the velocity shear scale length which depends on the system size and on the topology of the large-scale flow. In case of a circular monopole vortex [Fig. 1(c)], $L_s \approx L$. For the third moment, we compare $\langle(\delta v)^3\rangle \cong \epsilon r$ with the cross-correlation term $\langle \delta V(\delta v)^2\rangle \cong srC(\epsilon r)^{2/3}$ and observe that the influence of δV extends to a much smaller scale $l_* \cong C^{-3/2} s^{-3/2} \epsilon^{1/2}$, because the Kolmogorov constant C is larger than unity. Thus in the mesoscale range the second velocity moment may not be affected. As a result the spectrum may show $k^{-5/3}$ power law, while the third moment S_3 can be substantially modified, such that even its sign can reverse, as seen in Fig. 7(b).

D. Strong condensate

Here we consider the effect of an even stronger condensate vortex produced in a smaller boundary box of $L = 0.1$ m and at $\alpha = 0.05$ s^{-1}. The condensate strength parameter in these conditions is higher than in the intermediate condensate regime, $A = 0.78$. A single vortex is formed which then persists in the steady state. The energy spectrum after the subtraction of the mean flow is shown in Fig. 11(a). The spectral energy in the range of the wave numbers $k < 400$ m^{-1} is reduced compared to the values expected from the $k^{-5/3}$ trend. This phenomenon has been previously studied.[17] It has been found that the reduction in the spectral energy at low k is consistent with the mechanism of the shear decorrelation of turbulent eddies.

The third-order structure function $S_3(r)$, computed after subtracting mean flow, is shown in Fig. 11(b). It is positive in the range of scales up to the half-size of the boundary and it is a linear function of r. The energy flux deduced from S_3 gives $\epsilon = 9.2 \times 10^{-7}$ m^2 s^{-3}. This value is reasonably consistent with the energy dissipation rate of $\epsilon_c \approx 7 \times 10^{-7}$ m^2 s^{-3} derived from the energy decay.

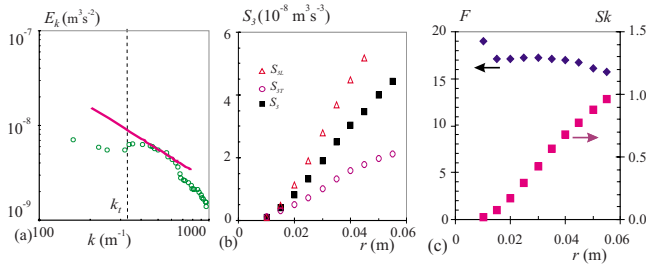

FIG. 11. (Color online) The strongest spectral condensate in the $L = 0.1$ m boundary box, linear damping $\alpha \approx 0.05$ s^{-1}, after mean subtraction. (a) Energy spectrum, (b) longitudinal (triangles), transverse (circles) and full (squares) third-order structure functions, and (c) flatness (diamonds) and skewness (squares) as functions of the separation distance r.

In the strong condensate regime the linear $S_3(r)$ dependence has the lowest scatter. This is easy to understand if we note that the values of skewness [squares in Fig. 11(c)] are much larger than in the cases of weak and intermediate condensates, $\mathrm{Sk} = (0.1-1)$. Larger skewness means stronger asymmetry in the probability distribution of δV^3, which makes it easier to detect in experiments with comparable statistics and reduces the scatter. The value of flatness is the highest in this regime, $F \approx 16$, also pointing to larger non-Gaussianity in the presence of strong spectral condensate.

Consistent with larger values of skewness, the value of the Kolmogorov constant in the strongest condensate regime is much smaller than in the previous two cases, $C \approx 1.8$, as estimated from the second-order structure constant C_{2L}. The Kolmogorov constant estimated as $C = E_k \epsilon^{-2/3} k^{5/3}$ from the spectrum is in the range of $C = 1.2-1.8$ in the energy cascade range. This value is closer to the value of the Kolmogorov constant in 3D turbulence. Thus the presence of the strong condensate substantially reduces the efficiency of the spectral energy transfer via the inverse cascade process.

IV. DISCUSSION AND SUMMARY

We reviewed previous and presented new experimental results (in particular, Figs. 1–3, 5, and 9–11) on the properties of spectrally condensed turbulence in thin layers of fluids. The accumulation of spectral energy at the box-size scale leads to the formation of a rather robust spectrum of the kinetic energy. This spectrum, along with the $k^{-5/3}$ (energy), and k^{-3} (enstrophy) inertial ranges of 2D turbulence, shows $E(k) \propto k^{-(3-4)}$ at large scales which appears due to the generation of a spectral condensate. The strength and the spectral extent of the condensate depend mostly on the scale-independent damping coefficient due to the bottom drag and on the box size in agreement with Ref. 18. The spectral condensate becomes a symmetric coherent vortex when the bottom dissipation rate α is decreased and $1/\alpha$ becomes comparable to, or larger than, the vortex turnover time. The radial

Downloaded 20 Dec 2009 to 150.203.179.95. Redistribution subject to AIP license or copyright; see http://pof.aip.org/pof/copyright.jsp

profile of the mean vorticity of the condensate vortex seems to be universal. It agrees with theoretical expectations and with the results of numerical simulation.[14]

In the reported experiments the energy dissipation is large in the inverse energy cascade range. Yet, many of the results presented in this paper, as well as in many previous experimental studies in thin stratified fluid layers and in the soap films, agree to certain extent with predictions of the 2D turbulence theory. The Reynolds numbers in our experiment are comparable with those in other experiments. The Taylor-microscale Reynolds number $R_\lambda = v_{\rm rms}\lambda/\nu$ can be estimated using the mean energy density and enstrophy of the flow, where the Taylor microscale $\lambda = (E/\Omega)^{1/2}$, $v_{\rm rms} = E^{1/2}$, and $\nu = 10^{-6}$ m^2 s^{-1}. In our experiments, R_λ is between 40 and 70, which is close to the value obtained in the soap film experiments[34] and in the "high" Reynolds number range as defined in numerical simulations.[35] The Reynolds number can also be estimated as $\mathrm{Re} = (1/\nu)\sqrt{C}\epsilon^{1/3}k^{-4/3}$, which for the conditions of the weak condensate gives (in the inverse cascade range at $k \approx 210$ m^{-1}) $\mathrm{Re} \approx 100$. In other words, the presence of substantial dissipation in the energy cascade range does not stop the cascade and does not significantly change statistical moments of turbulent velocity fluctuations.

We studied three regimes related to the condensate strengths of $A = E_{\rm cond}/E_0 = (0.2–0.78)$:

(i) In the weak condensate regime, $A \approx (0.2–0.4)$, statistical moments of turbulent velocity fluctuations are in agreement with the theoretical predictions and with the results of numerical simulations of 2D turbulence.

(ii) An intermediate condensate ($A \approx 0.61$) modifies velocity moments, however, the subtraction of time-average (mean) velocity field from the instantaneous fields recovers the second (spectra) and the third (S_3) velocity moments which appear similar to those in isotropic 2D turbulence. The Kolmogorov constant in this regime is close to its value of $C \approx 6$ in isotropic 2D turbulence. The fourth normalized moment, or flatness, increases in the presence of the mean shear flow from $F \approx 3$ in isotropic case, to $F \approx 5.5$ in the presence of an intermediate condensate.

(iii) A strong self-generated mean flow ($A \approx 0.78$) affects the efficiency of the inverse energy cascade as manifested by the lower value of the Kolmogorov constant in this regime, $C < 2$. The spectral condensate leads to shearing of the large-scale turbulent eddies and to the further increase in flatness, up to $F \approx 16$. It is likely that the increase in F is due to the shear suppression of eddies: the condensate shear distorts vortices whose vorticity is less than the external shear. Therefore strong (small-scale) vortices are affected by the condensate less than the vortices of a mean level, which increases F.

Perhaps, among the most surprising findings is the universality of the Kolmogorov flux relation in our experiments. The presence of a spectral condensate does not seem to affect the relationship between the third-order structure function and the energy flux in the inverse cascade range. The flux thus deduced is found to be in agreement with the energy dissipation rate derived from the energy decay after turning off forcing. This was confirmed in both weak condensate (largest bottom drag) and in the strongest condensate regime.

ACKNOWLEDGMENTS

We are grateful to V. V. Lebedev and G. Boffetta for useful discussions. We also thank E. Lindborg for his criticism which led to the clarification of several results in the paper including the effects of damping and the value of the Kolmogorov constant. We gratefully acknowledge contributions by H. Punzmann and D. Byrne at various stages of the experiment and thank M. Gwynneth for his many improvements of the experimental setup. This work was supported by the Australian Research Council Discovery Projects funding scheme (Grant No. DP0881544), Israeli Science Foundation (Grant No. 671/09), and Minerva Einstein Center.

[1] R. Kraichnan, "Inertial ranges in two-dimensional turbulence," Phys. Fluids **10**, 1417 (1967).
[2] J. Paret and P. Tabeling, "Experimental observation of the two-dimensional inverse energy cascade," Phys. Rev. Lett. **79**, 4162 (1997).
[3] J. Paret and P. Tabeling, "Intermittency in the two-dimensional inverse cascade of energy: Experimental observations," Phys. Fluids **10**, 3126 (1998).
[4] M. E. Maltrud and G. K. Vallis, "Energy spectra and coherent structures in forced two-dimensional and beta-plane turbulence," J. Fluid Mech. **228**, 321 (1991).
[5] G. Boffetta, A. Celani, and M. Vergassola, "Inverse energy cascade in two-dimensional turbulence: Deviation from Gaussian behavior," Phys. Rev. E **61**, R29 (2000).
[6] A. S. Monin and A. M. Yaglom, *Statistical Fluid Mechanics* (MIT, Cambridge, 1975), Vol. 2.
[7] V. Yakhot, "Two-dimensional turbulence in the inverse cascade range," Phys. Rev. E **60**, 5544 (1999).
[8] E. Lindborg, "Can the atmospheric kinetic energy spectrum be explained by two-dimensional turbulence?" J. Fluid Mech. **388**, 259 (1999).
[9] M. Hossain, W. H. Matthaeus, and D. Montgomery, "Long-time states of inverse cascades in the presence of a maximum length scale," J. Plasma Phys. **30**, 479 (1983).
[10] L. Smith and V. Yakhot, "Bose condensation and small-scale structure generation in a random force driven 2D turbulence," Phys. Rev. Lett. **71**, 352 (1993).
[11] L. Smith and V. Yakhot, "Finite-size effects in forced two-dimensional turbulence," J. Fluid Mech. **274**, 115 (1994).
[12] T. Dubos, A. Babiano, J. Paret, and P. Tabeling, "Intermittency and coherent structures in the two-dimensional inverse energy cascade: comparing numerical and laboratory experiments," Phys. Rev. E **64**, 036302 (2001).
[13] D. Molenaar, H. J. H. Clercx, and G. J. F. van Heijst, "Angular momentum of forced 2D turbulence in a square no-slip domain," Physica D **196**, 329 (2004).
[14] M. Chertkov, C. Connaughton, I. Kolokolov, and V. Lebedev, "Dynamics of energy condensation in two-dimensional turbulence," Phys. Rev. Lett. **99**, 084501 (2007).
[15] J. Sommeria, "Experimental study of the two-dimensional inverse energy cascade in a square box," J. Fluid Mech. **170**, 139 (1986).
[16] M. G. Shats, H. Xia, and H. Punzmann, "Spectral condensation of turbulence in plasmas and fluids and its role in low-to-high phase transitions in toroidal plasma," Phys. Rev. E **71**, 046409 (2005).
[17] M. G. Shats, H. Xia, H. Punzmann, and G. Falkovich, "Suppression of turbulence by self-generated and imposed mean flows," Phys. Rev. Lett. **99**, 164502 (2007).
[18] H. Xia, H. Punzmann, G. Falkovich, and M. G. Shats, "Turbulence-condensate interaction in two dimensions," Phys. Rev. Lett. **101**, 194504 (2008).
[19] S. Chen, R. E. Ecke, G. L. Eyink, M. Rivera, M. Wan, and M. Xiao, "Physical mechanism of the two-dimensional inverse energy cascade," Phys. Rev. Lett. **96**, 084502 (2006).
[20] R. A. D. Akkermans, L. P. J. Kamp, H. J. H. Clercx, and G. J. F. van

Downloaded 20 Dec 2009 to 150.203.179.95. Redistribution subject to AIP license or copyright; see http://pof.aip.org/pof/copyright.jsp

Heijst, "Intrinsic three-dimensionality in electromagnetically driven shallow flows," Europhys. Lett. **83**, 24001 (2008).
[21]S. Sukoriansky, B. Galperin, and A. Chekhlov, "Large scale drag representation in simulations of two-dimensional turbulence," Phys. Fluids **11**, 3043 (1999).
[22]S. Danilov and D. Gurarie, "Forced two-dimensional turbulence in spectral and physical space," Phys. Rev. E **63**, 061208 (2001).
[23]V. Borue, "Inverse energy cascade in stationary two-dimensional homogeneous turbulence," Phys. Rev. Lett. **72**, 1475 (1994).
[24]E. Lindborg, "Comment on 'Turbulence-condensate interaction in two dimensions'," Phys. Rev. Lett. **102**, 149401 (2009).
[25]G. D. Nastrom, K. S. Gage, and W. H. Jasperson, "Kinetic energy spectrum of large- and mesoscale atmospheric processes," Nature (London) **310**, 36 (1984).
[26]D. K. Lilly, "Two-dimensional turbulence generated by energy sources at two scales," J. Atmos. Sci. **46**, 2026 (1989).
[27]K. S. Gage and G. D. Nastrom, "Theoretical interpretation of atmospheric wavenumber spectra of wind and temperature observed by commercial aircraft during GASP," J. Atmos. Sci. **43**, 729 (1986).
[28]G. Falkovich, "Inverse cascade and wave condensate in mesoscale atmospheric turbulence," Phys. Rev. Lett. **69**, 3173 (1992).
[29]J. Y. N. Cho and E. Lindborg, "Horizontal velocity structure functions in the upper troposphere and lower stratosphere 1: Observations," J. Geophys. Res. **106**, 10223, doi:10.1029/2000JD900814 (2001).
[30]E. Gkioulekas and K.-K. Tung, "Recent developments in understanding two-dimensional turbulence and the Nastrom–Gage spectrum," J. Low Temp. Phys. **145**, 25 (2006).
[31]G. Brethouwer, P. Billant, E. Lindborg, and J.-M. Chomaz, "Scaling analysis and simulation of strongly stratified turbulent flows," J. Fluid Mech. **585**, 343 (2007).
[32]K. S. Smith, "Comments on 'The k^{-3} and $k^{-5/3}$ energy spectrum of atmospheric turbulence: Quasigeostrophic two-level model simulation'," J. Atmos. Sci. **61**, 937 (2004).
[33]K. K. Tung and W. W. Orlando, "The k^{-3} and $k^{-5/3}$ energy spectrum of atmospheric turbulence: Quasigeostrophic two-level model simulation," J. Atmos. Sci. **60**, 824 (2003).
[34]M. Rivera, P. Vorobieff, and R. Ecke, "Turbulence in flowing soap films: velocity, vorticity, and thickness fields," Phys. Rev. Lett. **81**, 1417 (1998).
[35]J. R. Chasnov, "On the decay of two-dimensional homogeneous turbulence," Phys. Fluids **9**, 171 (1997).

Downloaded 20 Dec 2009 to 150.203.179.95. Redistribution subject to AIP license or copyright; see http://pof.aip.org/pof/copyright.jsp